A Computational Model of the Dopaminergic and Pharmacological Modulations in the Subthalamopallidal Network of the Basal Ganglia

Ashra Roshy

Received December 17, 2024
Accepted March 19, 2025
Electronic access April 30, 2025

The basal ganglia, a complex network of interconnected subcortical nuclei, plays a critical role in motor control, cognition, and reward processing. Among its key circuits, the subthalamopallidal network—which includes the globus pallidus and the subthalamic nucleus– and the external modulator dopaminergic substantia nigra pars compacta—coordinates neural activity crucial for maintaining functional balance. This study focuses on computationally modeling the subthalamopallidal network and the substantia nigra pars compacta to elucidate its neuronal interactions, specifically investigating how the dopaminergic modulation of the substantia pars compacta and the various ion channels involved in the network affect network dynamics. Simulations reveal that excitation of the substantia nigra pars compacta are essential for maintaining structured behavior (stabilizing firing) and activity levels across the network. Manipulations of T-type low voltage-activated calcium channels highlight their pivotal role in regulating neuronal excitability and maintaining network cohesion, identifying them as potential pharmacological targets for neurodegenerative diseases like Parkinson's. Additionally, despite significant alterations to other ion channels and the introduction of progressive neuronal dysfunction, the subthalamopallidal network displayed robust compensatory mechanisms as deviations in structured behavior were in response to substantial modifications of network properties. These findings contribute to a greater understanding of basal ganglia circuitry and shed light on how ion channels influence both individual neuron behavior and network-wide dynamics in the human brain.

Introduction

The basal ganglia are a cluster of subcortical nuclei in the cerebral cortex[1] that moderate brain activity. The interactions of nuclei form a complex network named for its feedback loop structure: the basal ganglia circuit. Through intrinsic relationships and external influence, the basal ganglia circuit participates in motor control, executive functions, cognition, learning, and the reward-pleasure circuit[1].

The regulation of activity in basal ganglia cortical areas and their pathways is primarily performed by the neurotransmitter dopamine. Parkinson's disease occurs when the progressive loss of dopaminergic neurons in the substantia nigra pars compacta over-excites one pathway and over-inhibits another[2]. While dopaminergic modulation has been extensively researched, its full mechanisms remain unclear due to its complexity. Understanding this modulation could provide insights into neurodegenerative disorders and inform future therapies.

The subthalamopallidal network is a subcircuit of the basal ganglia circuit connecting the subthalamic nucleus and the globus pallidus externa[3]. This network is of interest due to the roles of these brain areas in motor control and their relevance in neurodegenerative disorders such as Parkinson's disease[4] and Huntington's disease. Although it only connects three brain areas, reducing complexity from its parent circuit, the neurophysiology and synaptic connections within the network are still being explored (for example, the nature of connections between the subthalamic nucleus and the globus pallidus externa in diseased individuals). However, the substantia nigra pars compacta has been identified as playing a key role in dopaminergic modulation. These factors make the subthalamopallidal network an optimal choice for further study.

Laboratory techniques to study network behavior face experimental limitations. Electrophysiology, which records electrical signals via electrode insertion, is commonly used[5]. While it provides real-time measurement, its invasiveness may cause tissue damage, affecting brain function. Additionally, electrophysiological data may offer only a partial view of network dynamics, limiting analysis. Computational methods do not face these constraints; their flexibility allows for efficient parameter adjustments and detailed analysis. While computational models cannot fully replicate the complexity of the real subthalamopallidal network, they are useful for preliminary studies.

This study aims to computationally model the subthalamopallidal network and visualize the effects of dopaminergic modulation on firing behavior and frequency. In addition to analyzing dopaminergic effects, this study seeks to identify other factors that contribute to maintaining regulated network behavior.

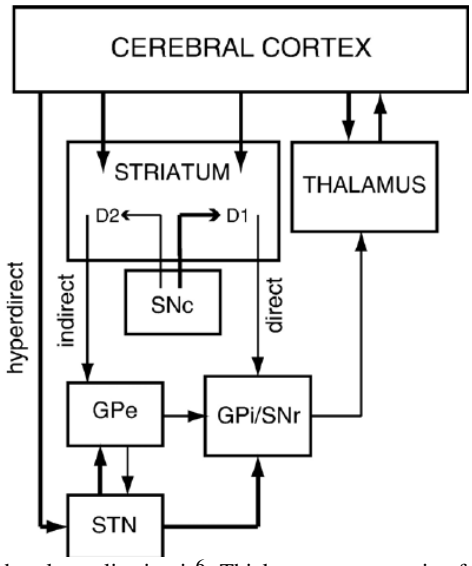

Fig. 1 The basal ganglia circuit[6]. Thick arrows connecting from box to box represent excitatory synaptic input. Thinner arrows connecting from box to box represent inhibitory synaptic input.

The Basal Ganglia

The Circuitry

The basal ganglia circuit is a closed loop that maintains strong communication between components that initiate and receive input from each other in tandem.

Initiation of behavior starts at the outermost layer of the brain, the cortex, and travels inward and outward as information is sent and received (Figure 1). In the basal ganglia network, the cortex projects to the basal ganglia. The entire neuroanatomy of the basal ganglia has not yet been established and is currently being explored. Several key regions include: the globus pallidus, subthalamic nucleus, and substantia nigra.

Globus Pallidus

The globus pallidus is a subcortical structure consisting of an internal segment (GPI) and an external segment (GPE). The globus pallidus receives most inhibitory input from the dorsal striatum[7] and sends inhibitory information to the subthalamic nucleus. Both the GPI and GPE are being explored for their role in Parkinson's disease.

Subthalamic Nucleus (STN)

The STN receives inhibitory GABAergic input from the GPE and sends excitatory current to the GPI and substantia nigra pars reticulata. The excitatory current sent to the GPI causes decreased activity in the thalamus and inhibition of movement[8]. The STN is highly correlated with proper control of movement[8].

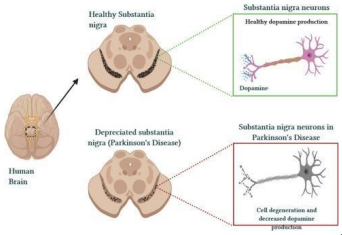

Fig. 2 Diseased SN neurons in the Parkinson's brain[9]. Top left, healthy SN. Bottom left, unhealthy SN. Top left, healthy nigra neuron with substantial dopamine (blue dots at synapse). Bottom right, diseased SN with low dopamine.

Substantia Nigra (SN)

The SN is composed of two parts: the substantia nigra pars compacta (SNc) and the substantia nigra pars reticulata (SNR). The SNc contains dopaminergic neurons that project to the striatum. The SNR, conversely, sends signals to the thalamus and brainstem, in conjunction with the GPI, as an output nucleus.

The loss of dopaminergic neurons in the SNc (Figure 2) is highly correlated with Parkinson's symptoms due to low dopamine levels decreasing proper signaling in the basal ganglia.

Dopaminergic Pathways

Two groups of neurons in the dorsal striatum are heavily involved in the basal ganglia circuit: D1-family dopamine receptor neurons, which produce an excitatory effect when exposed to dopaminergic SNc input, and D2-family dopamine receptor neurons, which produce an inhibitory effect[1]. The direct pathway primarily involves D1-expressing MSNs, GPi, and SNr, while the indirect pathway primarily involves D2-expressing MSNs and GPe (Figure 3). The hyperdirect pathway bypasses the striatum, involving the cerebral cortex, STN, GPi, and SNr. Although traditionally categorized by receptor type, some MSNs may express both D1 and D2[10], suggesting additional modulatory circuits beyond this model.

Disruptions in normal dopamine level can lead to severe neurological movement-based disorders and cognitive dysfunction by destroying circuit signalling.

In Parkinson's disease, reduced dopamine levels result in weaker inhibition from the striatum to the GPi and SNr, causing excessive thalamic inhibition (Figure 4). In the indirect pathway, increased inhibition of the GPe leads to over-excitation of the STN, further increasing GPi activity. The result—excessive inhibition of the thalamus—manifests as tremors, muscle stiffness, and slow movement[13]. Proper dopaminergic modulation prevents these dysfunctions by maintaining balanced basal ganglia influence on behavior.

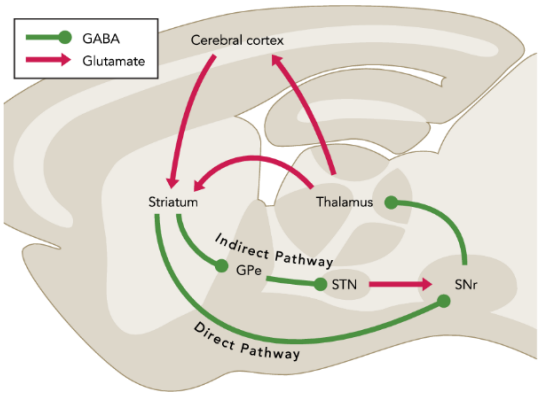

Fig. 3 Diagram of the direct and indirect pathway in the basal ganglia [11]. Green lines, GABAergic current; Red arrows , glutamatergic current.

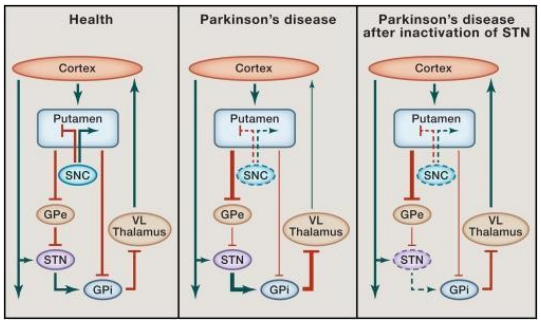

Fig. 4 Differences in pathway input for a normal subject and a Parkinson's subject [12]. Green arrows, excitatory current (arrow at projected target area); red lines, inhibitory current (dash at the projected target area). Line thickness corresponds to level of excitation or inhibition.

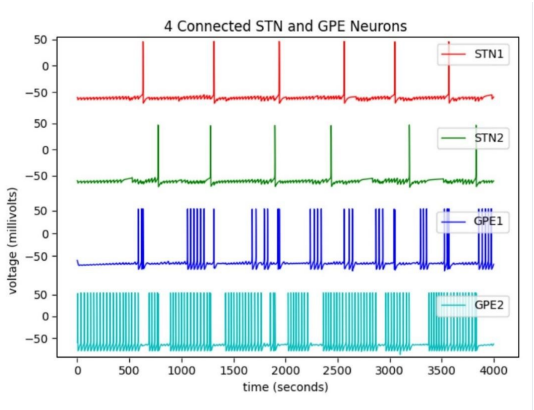

Fig. 5 Sparse-irregular behavior in STN and GPE neurons. Synaptic conductance values: $g_{G->S} = 0.5$, $g_{S->G} = 0.72$, and $g_{G->G} = 0.02$. Applied current was -1 pA. COV of STN1 = 1.40; COV of STN2 = 2.03.

The Subthalamopallidal Network

The subthalamopallidal network is a segment of the basal ganglia circuit that connects projection neurons in the globus pallidus and STN [3]. External dopaminergic SNc neurons signal the striatum, which inhibits GPE neurons in the indirect pathway and GPI neurons in the direct pathway. GPE and GPI neurons provide GABAergic input to STN neurons [14] which send excitatory AMPA-mediated signals back to the globus pallidus [15]. The STN excites GPI, which then inhibits the thalamus, relaying signals to the motor cortex. In this simplified model, SNc neurons act as relays without receiving synaptic input.

Results

Firing Behavior Differences in the GPE-STN Network

When GPE and STN neurons are first integrated into the subthalamopallidal network, two main types of overall network behavior become apparent: sparse-irregular firing, with a coefficient of variation (CV) ¿ 1 and infrequent spikes, and continuous-clustering behavior, with CV ¡ 1 and higher firing frequencies [16].

STN sparse-irregular behavior (Figure 5) is rare in healthy neurons and is linked to disorders like schizophrenia [17]. To generate continuous-clustering behavior characteristic of a healthy network, GPE-to-STN synaptic conductance was increased from 0.5 to 15, inducing STN bursting through sustained inhibition.

Connected STN neurons produced 12–15 spikes per burst over 400 milliseconds (Figure 6, top two traces), showing strong rebound spiking. GPE1 and GPE2 (Figure 6, bottom traces) fired in coordination with STN1 and STN2 inhibition, consistent with their inhibitory connection.

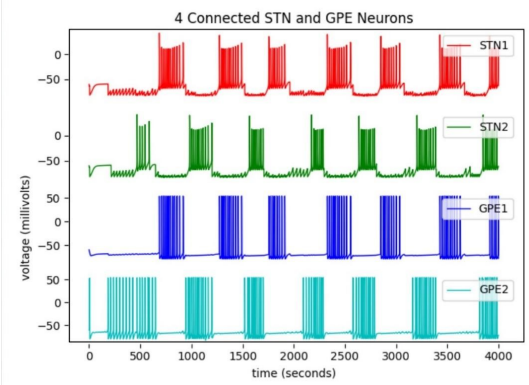

Fig. 6 Continuous-clustering behavior in STN and GPE neurons. Synaptic conductance values: $g_{G->S} = 15$, $g_{S->G} = 0.72$, and $g_{G->G} = 0.02$. Applied current was -1 pA. COV of STN1 = 0.42. COV of STN2 = 0.47.

SNc Excitation in the SNc-GPE-STN Network

Connecting SNc neurons to the subthalamopallidal network to form a twenty-seven circuit that offers deeper insight into basal ganglia internal dynamics.

With the application of a positive 15 pA to the network, the SNc neurons induced significant changes in GPE and STN firing behavior. SNc neuron firing (Figure 7a) triggered heightened firing of 36 Hz in the GPE neurons (Figure 7b) with interspike intervals of 50-100 milliseconds. In contrast, the STN neurons (Figure 7c) fired at around 8-8.5 Hz and lost more continuous-clustering behavior (STN COV = 0.66 as compared to STN COV = 49) with only occasional clusters of double or triple spikes.

Pharmacological Blockers in the Subthalamopallidal Network

Modifications in ion channel conductance values in the subthalamopallidal network simulated the effects of pharmacological blockers. When setting the sodium conductance to zero for STN and SNc neurons, SNc firing ceased instantly (Figure 8a) and STN firing became abnormal/spasmodic with an average firing rate of 10.8 Hz (Figure 8c) However, GPE neurons fired with an average frequency of 0.020 Hz (Figure 8b) — more so than when the sodium conductance of the STN and SNc neurons were set to standard conductance values (Table 1). This is likely due to intrinsic GPE properties maintaining its firing even without the excitatory current from synaptic connections with the STN and SNC neurons.

Computationally blocking the T-type low voltage-activated calcium ion channel demonstrated a greater dependence. When the T-type calcium channel was set to zero in only the GPE neurons (one-third of the network), 4 out of 9 STN neurons failed to reach the threshold, while the remaining neurons only fired 1 or 2 times through the entire 2000 milliseconds interval

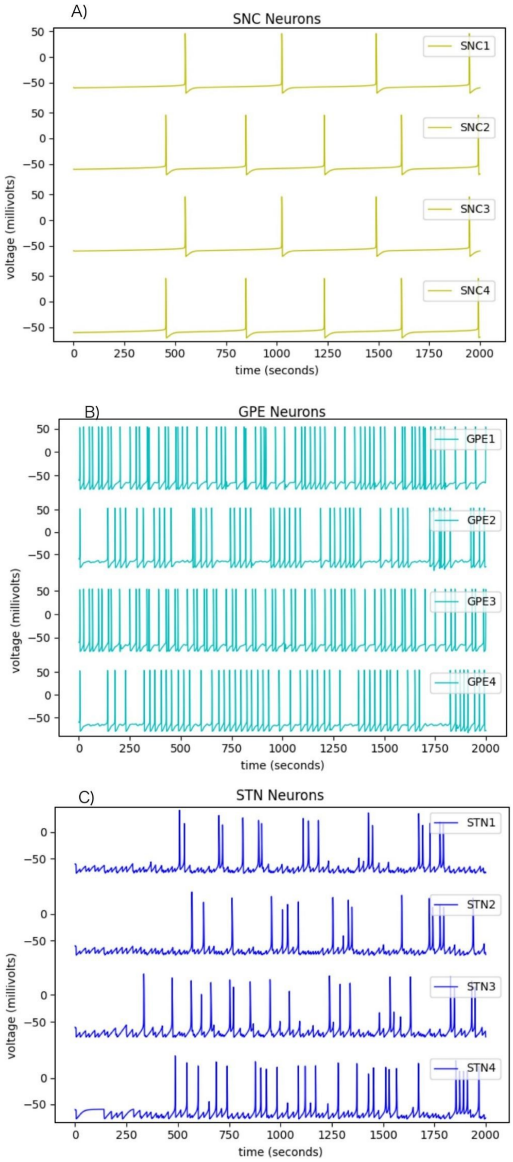

Fig. 7 Subthalamopallidal Network with an applied current of 15 pA given to five SNc neurons. Synaptic conductance values: $g_{G->S} = 3$, $g_{S->G} = 0.5$, and $g_{G->G} = 0.02$. Figure 7a. Four SNc neurons. Figure 7b. Four GPE neurons. Figure 7c. Four STN neurons.

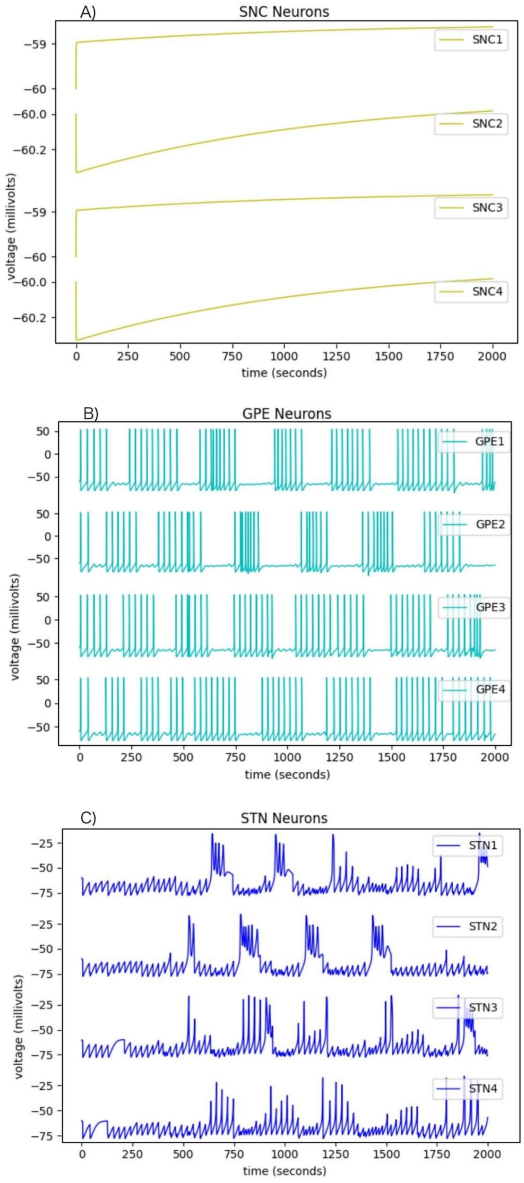

Fig. 8 The sodium conductance for the STN and SNc neurons was set to 0. Synaptic conductance values: $g_{G->S} = 3$, $g_{S->G} = 0.5$, and $g_{G->G} = 0.02$. Applied current was 3 pA. Figure 8a. SNc neurons. Figure 8b. GPE neurons. Figure 8c. STN Neurons

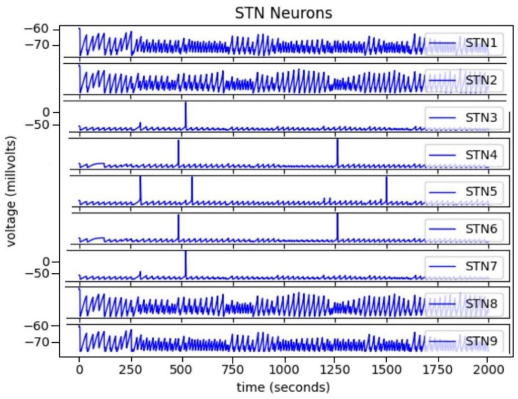

Fig. 9 Connected STN Neurons: GPE gT conductance set to zero. Synaptic conductance values: $g_{G->S} = 3$, $g_{S->G} = 0.5$, and $g_{G->G} = 0.02$. Applied current was 3 pA.

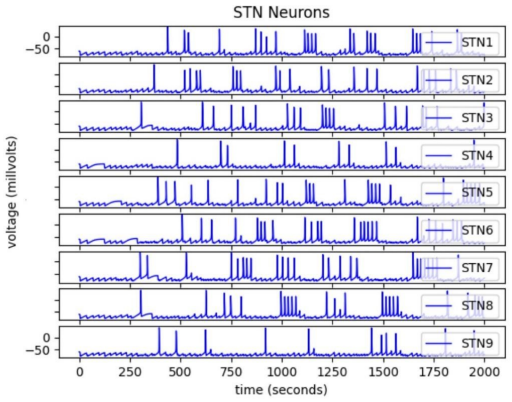

Fig. 10 Connected STN Neurons- GPE2 neuron IT ion current set to 0. Synaptic conductance values: $g_{G->S} = 3$, $g_{S->G} = 0.5$, and $g_{G->G} = 0.02$. Applied current was 3 pA.

(Figure 9).

When the T-type current was set to zero in just one neuron of the twenty-seven-neuron model, STN firing resumed. However, even the most active STN neurons, like STN6 and STN8, only fired three to four bursts before reverting to non-firing behavior (Figure 10). Since STN neurons rely on inhibitory input from GPe neurons for rebound bursting, the loss of T-type calcium channel activity in a single GPe neuron disrupts the strong rhythmic inhibition GPe provides to the STN [18].

The other calcium channel, the high-voltage-activated calcium channel, was examined for its impact on network behavior: the channel of a GPE neuron and a SNc neuron were blocked.

Although the amount of rebound firing decreased, nearly all neurons in the network—whether the calcium current of the GPE or SNc neuron was erased—continued to exhibit rebound bursts (Figure 11). These bursts predominantly consisted of quadruples to sextuples of spikes, aligning with the healthy continuous clustering behavior of the STN neurons.

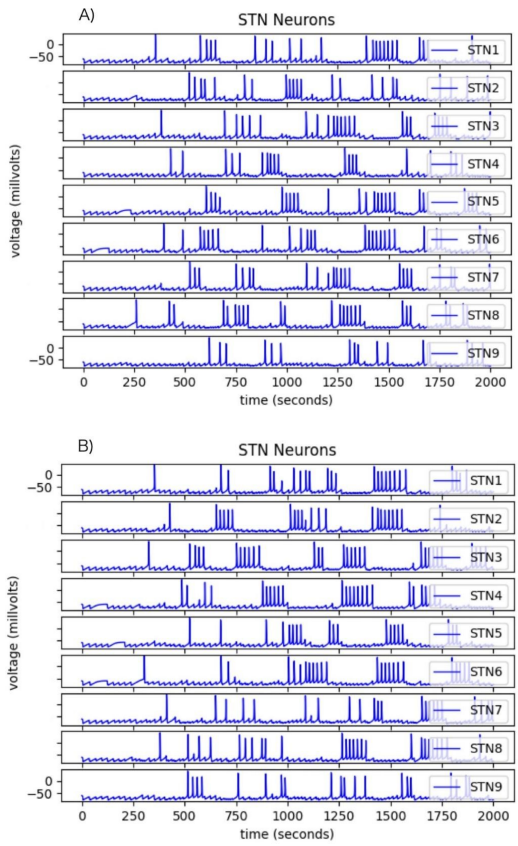

Fig. 11 Connected STN Neurons: Deadening a single Ca high voltage-activated ion channel in the subthalamopallidal network. Synaptic conductance values: $g_{G->S} = 3$, $g_{S->G} = 0.5$, and $g_{G->G} = 0.02$. Applied current was 3 pA. Figure 11a. STN neurons - GPE2 neuron Ca channel set to 0. Figure 11b. STN neurons - SNc9 neuron Ca channel set to 0.

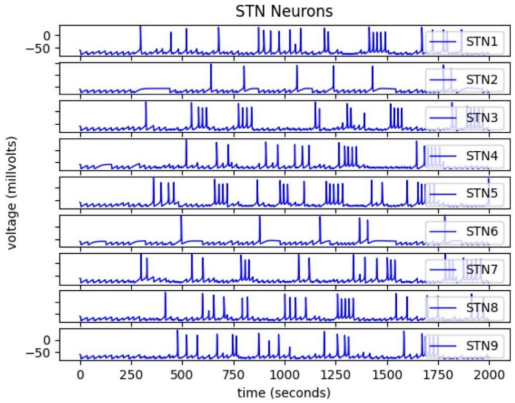

Fig. 12 Connected STN Neurons: 1 GPE neuron set to zero millivolts. Synaptic conductance values: $g_{G->S} = 3$, $g_{S->G} = 0.5$, and $g_{G->G} = 0.02$. Applied current was 3 pA.

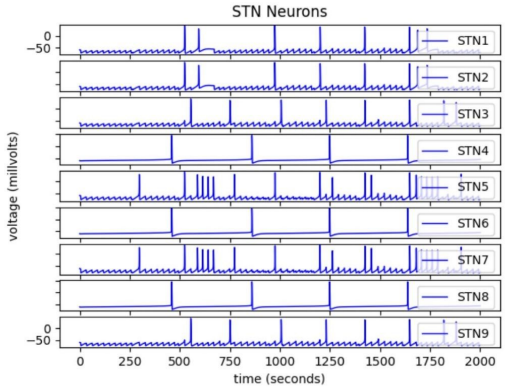

Fig. 13 Connected STN Neurons: 5 GPE neurons were set to zero millivolts. Synaptic conductance values: $g_{G->S} = 3$, $g_{S->G} = 0.5$, and $g_{G->G} = 0.02$. Applied current was 3pA.

Silenced Neurons in the Subthalamopallidal Network

To assess how the SNc's dopaminergic modulation could potentially resist membrane voltage alterations of network components, the GPE neurons were sequentially set to zero millivolts.

Although two STN neurons lost their ability to exhibit rebound firing completely and provided minimal signaling to other neurons in the network, most of the remaining STN neurons continued to display rebound bursting behavior, firing four to six times during these bursts (Figure 12). The input of the remaining GPE input and dopaminergic SNc were able to withstand the 'deletion' of a single GPE neuron. When five GPE neurons—more than half of the GPE population—were 'deadened' (Figure 13), STN neurons presented little rebound firing and low frequencies (1-2.5 Hz).

However, despite silencing the majority of GPE neurons in the computational network, the STN neurons still continued to

fire (albeit weakly).

Discussion

The complexity of the basal ganglia circuit is still not fully uncovered. To analyze its connections, a computational model of the subthalamopallidal network was created. Based on "Activity Patterns in a Model for the Subthalamopallidal Network of the Basal Ganglia"[3], model neurons replicated the neuronal properties and firing behaviors of the STN, GPE, and SNc.

Dopaminergic modulation was indirectly modeled through changes in SNc firing frequency, controlled by applied current. Excitatory connections from SNc to GPE linked the SNc to the rest of the model. Visualizing the network showed that SNc firing changes caused detrimental increases or decreases in GPE and STN firing. SNc firing also helped compensate for membrane voltage losses of other network components (GPe neurons), allowing STN neurons to maintain their continuous-clustering behavior. Only moderate SNc firing preserved the continuous-clustering behavior of the subthalamopallidal network, emphasizing the importance of dopaminergic modulation.

The network remained stable even when pharmacological blockers and neurobiological changes were simulated. Three ion channels were tested for their role in network stability: the sodium channel, T-type calcium channel, and high voltage-activated calcium channel. Alterations showed a greater deterioration with the loss of T-type calcium current, due to its role in rebound spiking and rhythmic firing. As T-type channels are essential for action potential initiation at low membrane potentials, especially after inhibition, neurons failed to reach the threshold for rebound spiking— leading to impaired firing patterns. These disruptions in timing and synchronization affected network activity, as precise firing is crucial for communication and function. Simulating neuronal death by progressively setting neuron voltages to zero had minimal effects on network behavior until five GPE neurons were silenced, at which point structured rebound firing and signaling in STN neurons deteriorated.

Overall, the computational subthalamopallidal network demonstrated robustness as it was able to maintain stability and firing even with alterations. Balanced excitatory-inhibitory interactions between the STN and GPe likely contributed to its robustness. The model's durability highlights the strength of the basal ganglia circuit; while the physical subthalamopallidal network consists of millions of neurons, its resistance to dysfunction prevents neurodegenerative disorders from being more prevalent.

Computational disruptions provided unexpected insights into neuron properties crucial for stability. One major finding was the T-type calcium channel's significant role in maintaining STN behavior and network structure, suggesting potential therapeutic avenues for neurodegenerative diseases like Parkinson's[19]. However, other stability mechanisms, such as synaptic plasticity—where excitatory or inhibitory synapses adjust strength—or homeostatic upregulation of ion channels, might also compensate for T-type calcium current loss[20].

The computational subthalamopallidal-SNc model remains a simplified representation of the biological network. Expanding the number of SNc, GPe, and STN neurons could reveal emergent properties absent in smaller networks. The exclusion of critical factors also likely impacted network dynamics. Excluding nonlinear synaptic interactions could have led to more consistent firing behavior not representative of true dynamics. Lack of neuronal heterogeneity may also have impacted network stability as excluded 'diseased' cells would significantly alter overall behavior. Lastly, excluding synaptic plasticity, allowing neurons to dynamically change connection strengths in response to alterations, might mean under-valuing of the true network's robustness. However, despite its limitations, the model successfully reproduced fundamental subthalamopallidal neuron behaviors observed in murine electrophysiological recordings[21].

Although further refinement is needed, these initial findings lay the groundwork for deeper exploration of the intricate basal ganglia circuitry.

Methods

Overview of the Model Network

The subthalamopallidal-SNc network consisted of nine GPE neurons, nine STN neurons, and nine SNc neurons modeled over 2000-4000 milliseconds to capture transient behavior and analyze the stable firing dynamics of the mode. All neurons were represented with initial conditions: V (-60 mV), s (0.001), n (0.001), h (0.01), r (0.01), and Ca^{2+} (0.01).

The STN Neuron Model

All ionic currents, conductances, and parameters were derived from "Activity Patterns in a Model for the Subthalamopallidal Network of the Basal Ganglia"[3]. Neuron behavior was given by the membrane Potential (V): $C_m \frac{dV}{dt} = -I_L - I_K - I_{\text{Na}} - I_T - I_{\text{Ca}} - I_{\text{AHP}} - I_{G\to S}$

The GPE Neuron Model

All ionic currents, conductances, and parameters were derived from *Activity Patterns in a Model for the Subthalamopallidal Network of the Basal Ganglia*[3]. Neuron behavior was given by the membrane potential V:

$C_m \frac{dV}{dt} = -I_L - I_K - I_{\text{Na}} - I_T - I_{\text{Ca}} - I_{\text{AHP}} - I_{S\to G} - I_{G\to G}$.

The low voltage-activated calcium current was simplified to $g_T a_\infty^3(V) r(V - V_{\text{Ca}})$,

where $\tau_r(V) = \tau_r$ to reduce rebound bursts.

Table 1 STN Model Parameters.

Parameter	Value
g_L	2.25
g_K	45
g_{Na}	37.5
g_T	0.5
g_{Ca}	0.5
g_{AHP}	9
v_L	-60
v_K	-80
v_{Na}	55
v_{Ca}	140
τ_h^1	500
τ_n^1	100
τ_r^1	17.5
τ_h^0	1
τ_n^0	1
τ_r	40
ϕ_h	0.75
ϕ_n	0.75
ϕ_r	0.2
k_1	15
k_{Ca}	22.5
ε	$3.75 * 10^{-5}$
θ_m	-30
θ_h	-39
θ_n	-32
θ_r	-67
θ_a	-63
θ_b	0.4
θ_s	-39
θ_h^τ	-57
θ_n^τ	-80
θ_r^τ	68
θ_g^H	-39
θ_g	30
α	5
$V_{G->S}$	-85
σ_m	15
σ_h	-3.1
σ_n	8
σ_r	-2
σ_a	7.8
σ_b	-0.1
σ_s	8
σ_h^τ	-3
σ_n^τ	-26
σ_r^τ	-2.2
σ_g^H	8
β	1

Table 2 GPE Model Parameters

Parameter	Value
g_L	0.1
g_K	30
g_{Na}	120
g_T	0.5
g_{Ca}	0.15
g_{AHP}	30
v_L	-55
v_k	-80
v_{Na}	55
v_{Ca}	120.0.
τ_h^1	0.27
τ_n^1	0.27
τ_h^0	0.05
τ_n^0	0.05
τ_r	30
ϕ_h	0.05
ϕ_n	0.05
ϕ_r	1
k_1	30
k_{Ca}	20
ε	1×10^{-4}
θ_m	-37
θ_h	-58
θ_n	-50
θ_r	-70
θ_a	-57
θ_s	-35
$\theta_h\tau$	-40
$\theta_n\tau$	-40
θ_g^H	-57
θ_g	20
α	2
$V_{G->G}$	-100
σ_n	10
σ_h	-12
σ_n	14
σ_r	-2
σ_a	2
σ_s	2
$\sigma_h\tau$	-12
$\sigma_n\tau$	-12
σ_g^H	2
β	0.08
$V_{S->G}$	0

The Model SNc Neuron

The SNc neuron model was given by: $C_m \frac{dV}{dt} = -I_L - I_K - I_{\text{Na}} - I_{Ca} - I_{\text{AHP}} - I_{\text{SNc}\to G} - I_{\text{App}}$. The low T-type calcium current

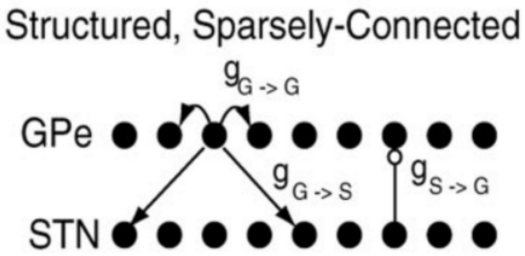

Fig. 14 Depiction of the structured, sparsely connected GPE-STN network[3]. Dots represent neurons: there are 9 GPE neurons and 9 STN neurons. Arrows represent inhibitory current. Lines with open circles at the end represent excitatory current. Not all connections are shown in the above figure.

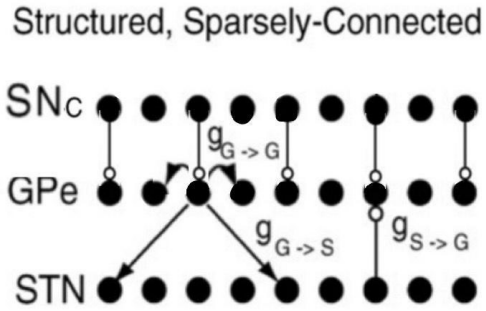

Fig. 15 Depiction of the structured, sparsely connected SNc-GPE-STN network[3].Not all connections are shown in the above figure, only some of them.

was omitted for simplicity, but it may have reduced SNc burst firing, caused irregular pacemaking, and decreased dopamine release/modulation compared to a biological SNc neuron.

Connecting the Network

The partial 18-neuron network, created before the addition of dopaminergic SNc neurons into the computational model, was connected in a structured and sparsely connected form (Figure 14). The GPE to STN conductance, STN to GPE conductance, and GPE to GPE conductance values, were set to 15, 0.72, and 0.02, respectively, to produce continuous clustering behavior. GPE neurons were given an applied current ($+I_{App}$).

Subsequently, the nine SNc neurons were connected in a one-to-one manner to create the 27-neuron subthalamopallidal network (Figure 15). Odd-numbered SNc neurons received an applied current, while the rest did not.

Acknowledgments

I would like to thank Professor Dr. Arij Daou, who guided me through this research paper.

References

1 C. B. Young and J. Sonne, 2023.

2 D. J. Surmeier, *FEBS Journal*, 2018, **285**, 3657–3668.

3 D. Terman, J. E. Rubin, A. C. Yew and C. J. Wilson, *Journal of Neuroscience*, 2002, **22**, 2963–2976.

4 C. D. Hardman, G. M. Halliday, D. A. McRitchie and J. G. Morris, *Journal of Neuropathology & Experimental Neurology*, 1997, **56**, 132–142.

5 P. Hoerbelt and B. D. Heifets, *Methods in Enzymology*, 2018, **602**, 301–338.

6 S. Tinaz, H. E. Schendan, K. Schon and C. E. Stern, *Brain Research*, 2006, **1067**, 239–249.

7 N. Javed and M. Cascella, 2022.

8 H. Basinger and J. Joseph, 2021.

9 P. Singh, N. Mishra, N. Singh, N. Alka, R. Nisha, P. Maurya, R. R. Pal and S. A. Saraf, 2022.

10 A. T. Allen, K. N. Maher, K. A. Wani, K. E. Betts and D. L. Chase, *Genetics*, 2011, **188**, 579–590.

11 A. V. Kravitz and A. C. Kreitzer, *Physiology*, 2012, **27**, 167–177.

12 H. Y. Zoghbi, *Cell*, 2014, **158**, 1225–1229.

13 A. Nair, A. Razi, S. Gregory, R. R. Rutledge, G. Rees and S. J. Tabrizi, *Brain*, 2021, **145**,.

14 J. P. Bolam, J. J. Hanley, P. A. Booth and M. D. Bevan, *Journal of Anatomy*, 2000, **196**, 527–542.

15 H. Nakanishi, H. Kita and S. T. Kitai, *Brain Research*, 1987, **437**, 35–44.

16 J. S. Taube, *Journal of Neurophysiology*, 2010, **104**, 1635–1648.

17 P. J. Uhlhaas and W. Singer, *Nature Reviews Neuroscience*, 2010, **11**, 100–113.

18 L. A. Koelman and M. M. Lowery, *Frontiers in Computational Neuroscience*, 2019, **13**, 77.

19 L. G. Matthews, C. B. Puryear, S. S. Correia, S. Srinivasan, G. M. Belfort, M. Pan and S. Kuo, *Annals of Clinical and Translational Neurology*, 2023, **10**,.

20 P. Bülow, T. J. Murphy, G. J. Bassell and P. Wen, *Cell Reports*, 2019, **26**, 1378–1388.

21 K. C. Loucif, C. L. Wilson, R. Baig, M. G. Lacey and I. M. Stanford, *Journal of Physiology*, 2005, **567**, 977–987.